Fuel 285 (2021) 119120

Contents lists available at ScienceDirect

Fuel

journal homepage: www.elsevier.com/locate/fuel

Investigation of wet combustion instability due to bio-syngas fuel variability

Kai Zhang *, Giandomenico Lupo, Christophe Duwig

Department of Chemical Engineering, Royal Institute of Technology (KTH), Sweden

ARTICLE INFO

Keywords:
Humidified gas turbine
Fuel variability
Uncertainty quantification
Flame instability

ABSTRACT

Humidified gas turbine (HGT) is a promising technology with several advantages compared to traditional thermal power plants, such as higher electrical efficiency, lower investment costs, and lower emissions. Using steam diluted, carbon neural bio-syngas as fuel in the HGT cycle leads to distributed wet combustion, often characterised by high Karlovitz number. This kind of combustion may be unstable if a small perturbation of bio-syngas fuel composition occurs and it can lead to flame blow-off. Hence, quantifying wet bio-syngas fuel variability effects on the flame physicochemical behaviour is an important step. Using uncertainty quantification, it is found that a 0.75% perturbation of a typical wet bio-syngas composition can lead to 10% fluctuation of the flame speed, 7.5% fluctuation of the flame thickness and 2% fluctuation of flame temperature for stoichiometric combustion of steam diluted reactants at gas turbine conditions. Since near stoichiometric combustion is associated with highly steam-diluted bio-syngas to retain constant thermal efficiency of HGT, ultra-wet combustion has indeed suffered from strong combustion instability led by fuel variability. The main sensitivity study shows that hydrogen variability is responsible for the high fluctuation of flame speed while methane variability is responsible for the fluctuation of thermal efficiency and flame thickness. A high pressure (HP) burner running on a typical wet bio-syngas can suffer from a change of Karlovitz number by 20 (300% by fraction) and Reynolds number by 14,000 (10% by fraction), with potential impact on flame stability and cycle performance due to small perturbation of bio-syngas composition.

1. Introduction

To cut down greenhouse gas emission in EU by at least 40% below 1990 level, European commission aims to improve share of renewable energy to at least 32% of final energy consumption and increase energy efficiency to 32.5% by 2030. Humidified gas turbine (HGT) technology has great potentials for combined heat and power (HCP) production, owing to its higher electrical efficiency up to 60% and lower investment costs compared to traditional steam turbines [1]. Several variations of the HGT cycle have been studied, mainly classified by how steam/liquid water is generated, injected, and condensed/evaporated within the cycle [2,3]. These variations may differ in terms of their capability to improve total, electrical, and heat efficiencies over existing dry gas turbine cycles. As a result, transforming existing power production lines to include HGT of different kind requires a systematic evaluation of investment costs and returns, which slows down the application of this relevant technology [4]. Recently, Phoenix Biopower AB in Sweden started on-site tests of using the gas products of high steam, high pressure biomass pyrolysis to produce carbon-free bio-power [5]. Pivotal towards the fulfilment of the promise to achieve 60% electrical efficiency in 2030, an HGT cycle in which steam is recirculated and used at various points of the whole process sits at the core of their so-called BTC (Biomass-fired TopCycle) power plant. Several difficulties are faced, amongst which more than 50% steam in reactants poses challenges to achieving stable combustion of the ultra-wet bio-syngas.

Specifically, ultra-wet bio-syngas combustion faces flame stabilisation issues at two levels. First, bio-syngas produced from different grades of biomass is often associated with fuel composition variability [6,7], which may change the flame behaviour during practical operation of HGT. The possible steps towards useful bio-syngas for gas turbine combustion are complex, starting from high pressure (HP) steam treated biomass pyrolysis, to biochar gasification, and finally to bio-syngas clean-up. Under some circumstances, when the biomass is over-wet before the HP steam treatment, an air dryer is also needed. Amongst these steps, the composition of the bio-syngas product, such as the H_2/CO/CH_4 ratio, may vary significantly, even when the most stable manners of control are applied [8]. In particular, the water–gas shift

* Corresponding author.
E-mail address: kaizhang@kth.se (K. Zhang).

https://doi.org/10.1016/j.fuel.2020.119120
Received 23 February 2020; Received in revised form 26 August 2020; Accepted 28 August 2020
Available online 25 September 2020

Nomenclature:

D_m	Mixing tube diameter (m)
E	Expectation
f_i	Deterministic sensitivity coefficient
Ka	Karlovitz number
L	Characteristic length (m)
P	Truncation order
Q, Q'	Flame quantity and its fluctuation
Re	*Reynolds number*
S_i	Main sensitivity index
S_{ij}	Join sensitivity index
S_L	Laminar flame speed (m/s)
T_{ad}, T_{in}	Adiabatic flame temperature, inlet temperature of mixture (K)
T_u, T_b	Unburnt and burnt mixture temperature
U_{bulk}	Bulk velocity (m/s)
u'	Velocity fluctuation (m/s)
Var	Variance
x_k	Mole fraction of each species k
BTC	Biomass-fired TopCyle
DM	Determinstic sampling method
HGT	Humidified gas turbine
HP	High pressure
HCP	Combined heat and power
LHS	Latin-Hypercube-Sampling
LHV	Lower heating value
MCS	Monte-Carlo sampling
ODE	Ordinary differential equation
PCE	Polynomial chaos expansion
PDF	Probability density function
UQ	Uncertainty quantification

Greek symbols

μ, μ_i	Nominal values, mean value of quantity i
σ_i	Standard deviation of quantity i
λ	Sample mass fraction
ξ	Quadrature points
w	Weights
η	Carnot efficiency
ϕ	Equivalence ratio
δ_L	Thermal flame thickness (m)
ν	Kinematic viscosity (m^2/s)
α_k^i	Degree of Legendre polynomial
Δk_i	Perturbation of rate constant of reaction i

reaction, whose kinetic rate is sensitive to temperature fluctuations in the gasifier, has a direct impact on the product gas composition.

As for the second flame stabilisation issue, highly steam-diluted bio-syngas combustion leads to high Karlovitz number (Ka), *i.e.*, potentially longer chemical reaction time compared to mixing time. Small eddies are able to penetrate into the reaction zone and take away heat rapidly. This indicates that wet combustion has a higher tendency to flame blow-off at operating conditions similar to traditional dry gas turbines and is therefore more sensitive to fuel variability. Although swirling flow may help the stabilization of a typical high Ka flame via increasing flame residence time [9], more research efforts are needed to understand the behaviour of swirl stabilised, ultra-wet bio-syngas flames. Moreover, ultra-wet combustion can also be stabilised by increasing the fuel/air ratio to approach stoichiometry. Less air excess and more steam involved to drive the gas turbine expander benefit the HGT efficiency, with risk for high CO emission. Despite many studies show that the CO level can be acceptable at practical high-pressure wet-combustion conditions [10-12], compromises are needed amongst the steam content, CO emissions, and flame stability. In the end, the second flame stabilisation issue is strongly coupled with the high Ka flame that can be easily extinguished due to a small perturbation of wet bio-syngas fuel composition.

Therefore, wet bio-syngas fuel variability poses great challenges to the integration of the ultra-wet combustion technique into the HGT cycle. Many researchers [13-15] have investigated the effect of high steam dilution on the H_2/CO flame physicochemical behaviour as these two species are the main components of syngas. Studies of steam diluted bio-syngas containing H_2/CO/CO_2/CH_4 are still scarce [16,17]. Meng *et al.* [13] measured the flame speed of H_2/CO burning in O_2/H_2O environment: the chemical effects of H_2O addition promotes H_2/CO combustion for H_2 content below 50%. A complex effect was noticed when a large amount of H_2O is added: the concentration of free radicals (O, H, OH) is decreased, partly via increase of three-body reactions such as $H + O_2(+M) = HO_2 + (M)$. This is primarily a result of the higher third body coefficient of H_2O compared to N_2 [18]. Xu *et al.* [14] performed experimental and numerical studies of H_2/CO diffusion flame also in O_2/H_2O environment. The chemical and thermal effects of H_2O on OH formation were reported to be more important compared to transport and radiative effects. Krejci et al. [15] discussed the steam dilution (0 ~ 15% by volume) effect on the laminar flame speed of syngas blends of different H_2/CO ratios at different temperatures (323 ~ 423 K). The flame speed of H_2-rich blends is more sensitive to steam dilution, while CO-rich blends experience less influence. Lee *et al.* [19] reviewed the combustion properties of practical bio-syngas H_2/CO/CO_2/CH_4 mixture compositions, relevant to lean-premixed, dry gas turbine cycles; fundamental properties of practical bio-syngas flames were reported, though steam dilution was not considered.

Despite these valuable results, there is a lack of knowledge about the likelihood of flame blow-off when highly steam-diluted bio-syngas is subject to a random small change of methane and hydrogen concentrations. If the bio-syngas composition is known, one can predict the HGT behaviour at given conditions, but small inevitable fuel uncertainties/variabilities are more difficult to handle. In 2018, one of the authors of the present study employed uncertainty quantification (UQ) for the first time to investigate the role of bio-syngas fuel (9.5%CH_4-35.5%CO-30.5H_2-25.5%CO_2) variability on the flame physicochemical properties [20]. A 0.75% variance of each of the three species CH_4/CO/H_2 leads to 14% flame speed fluctuation for rich combustion ($\phi = 1.8$) and 1.5% for lean combustion ($\phi = 0.6$) at 300 K and 1 atm. Hydrogen variability plays a significant role (70% to 80%) on producing the flame speed fluctuation, while methane impact is negligible. In another recent study of a fuel with different H_2/CO ratio, a similar result was observed, and it was concluded that the flame speed fluctuation is dominated primarily by the variability of H_2, followed by CO, CO_2, and CH_4 [21]. Very lean combustion ($\phi = 0.45$) with high H_2/CO fuel ratio containing a small compositional change of 0.75% variance, resulted in the highest flame speed fluctuation, of about 5%.

However, the steam effect on the fuel variability which causes wet combustion instability remains unexplored. Therefore, the present study aims to fill this gap by providing novel findings and discussions on 1) the general effect of steam content on wet combustion instability; 2) the sensitivity of flame physicochemical properties to the variability of renewable bio-syngas compositions; 3) how to reduce flame instability from upstream gasification. The present work is the first attempt to use UQ to understand wet combustion instability from the perspective of fuel variability.

The present study is structured as follows. Section 2 summarises the steps of the UQ method and introduces the new assumptions made to

improve its accuracy. Section 3 analyzes the results obtained and discusses the impact of flame fluctuations on practical HGT operation. Finally, conclusions are given in Section 4.

2. Methodologies

2.1. Background and polynomial chaos expansion

In the present study, UQ analysis is performed invoking the advantages of polynomial chaos expansion (PCE) based surrogate models which can replace ODEs describing one-dimensional flame features in the Cantera Package [22]. The PCE method was introduced by Wiener [23] and later widely used in combustion science to evaluate chemistry models [24-26]. The method conveniently expresses the variance-based sensitivity indices ('Sobol' indices [27]) as part of the constructed PCE model, such that the quantitative effect of the input variables of a dynamical system on the variance of the system output can be directly obtained [28]. A deterministic sampling method (DM), recognised to converge faster than conventional Monte-Carlo sampling (MCS [29]) and Latin-Hypercube-Sampling (LHS [30]), is often employed during the PCE model construction process when the PC coefficients must be evaluated using quadrature rules [31]. The details of the UQ method are described in previous publications [20,21]; hence only the key steps relative to the present case are summarised as:

Step 1: Pre-storage of the quadrature points ξ according to the polynomial type (Legendre), PCE dimensions D and truncation order of the expansion P.
Step 2: Representation of the sampled input variables λ with the quadrature points ξ.
Step 3: Calculation of target flame quantities Q using the sample variables λ.
Step 4: Galerkin projection to evaluate the PC coefficients using the chosen polynomial type with quadrature points ξ, weights w, and flame quantities Q.
Step 5: Expansion of the flame quantity Q on the chosen orthogonal polynomial basis.
Step 6: Forward propagation of the input variables through PCE to obtain the desired flame quantity Q.
Step 7: Analysis of the PCE using Sobol indices (PCE destruction) and construction of probability density functions (PDFs) for the flame quantity Q.

The composition of the chosen ultra-wet bio-syngas fuels is shown in Table 1. The low hydrogen and methane contents indicate that the investigated bio-syngas is of the type with very low heating value, produced from high-pressure steam treatment and gasification of biomass [5,32]. The species mole fractions, except for that of steam, are superscripted with 'dry' indicating that they are calculated on the dry basis and their sum is unity. The H_2O mole fraction, relative to the wet bio-syngas, is superscripted with 'wet'. The three cases differ mainly in terms of their methane content, whilst the ratio of $H_2/CO/CO_2$ is kept constant. The lower heating value (LHV) for cases 1, 2 and 3 is 3.94 MJ/Kg, 5.21 MJ/Kg, and 6.55 MJ/Kg respectively.

Table 1
Representative bio-syngas composition in mole fractions.

Case	Dry Bio-syngas Composition					Equivalence Ratio	Steam Content
	H_2^{dry}	CO^{dry}	CO_2^{dry}	CH_4^{dry}	N_2^{dry}	ϕ	H_2O^{wet}
1	0.093	0.176	0.224	0.050	0.457	0.6, 0.7, 0.8, 0.9, 1.0	0.25, 0.35, 0.41, 0.45, 0.47
2	0.084	0.158	0.201	0.100	0.457	0.6, 0.7, 0.8, 0.9, 1.0	0.35, 0.45, 0.51, 0.55, 0.57
3	0.074	0.140	0.179	0.150	0.457	0.6, 0.7, 0.8, 0.9, 1.0	0.43, 0.53, 0.58, 0.62, 0.64

The nominal species fractions of the bio-syngas in Table 1 are obtained from Phoenix Biopower [5], an industrial partner of the authors. Since the nominal concentrations of the species are associated with unavoidable small uncertainties, it is crucial to investigate if the HGT will still operate in a safe and efficient mode. A 0.75% variance, relative to the nominal value, is assumed for the dry species fractions, except for N_2. This is realized by sampling the dry species fractions from a uniform PDF, symmetric around the nominal value, with 1.5% support on either side. This is acceptable as there is a lack of evidence on how a practical PDF may look like.

The uncertain input variables are therefore calculated as:

$$\begin{cases} \lambda_1 = H_2^{dry} = \mu_1 + 0.015 \times \xi_1, \\ \lambda_2 = CO^{dry} = \mu_2 + 0.015 \times \xi_2, \\ \lambda_3 = CO_2^{dry} = \mu_3 + 0.015 \times \xi_3, \\ \lambda_4 = CH_4^{dry} = \mu_4 + 0.015 \times \xi_4; \end{cases} \quad (1)$$

where λ, μ and ξ are the sample mass fractions, nominal values and quadrature points defined in Step 2 above, and ξ is sampled in $[-1, 1]$ using quadrature rule. The PCE dimension D is therefore equal to 4.

The conditions examined in the present study differ from the ones used in the previous publications [20,21] mainly on two points. First, chemical reactions involving the inert species N_2 are ignored. Second, the flame temperature is pre-calculated at 1 atm and kept constant. These modifications are made in order to migrate the UQ method to practical cases. In HGT, high steam content is used as a heat carrier and working medium to control the combustor exit temperature and improve the turbine efficiency [2]. The combustor exit temperature T_b can be approximated with the adiabatic flame temperature T_{ad}, and the turbine (or thermal) efficiency η may be approximated with Carnot efficiency,

$$\eta = 1 - \frac{T_u}{T_b} = 1 - \frac{T_{in}}{T_{ad}} \quad (2)$$

where the unburnt mixture temperature T_u (or T_{in}) is assumed to be 780 K in the present case, a practical inlet temperature for the reactants in the HGT cycle. The adiabatic flame temperature is required to be stable and is often below 1700 K to reduce thermal NO_x emissions and to prevent downstream burn-out of the gas turbine expander.

For this reason, in the present study, ϕ and H_2O^{wet} are always associated, written as $\{\phi, H_2O^{wet}\}$, in order to always keep the adiabatic flame temperature at around 1720 K. Their values in Table 1 are pre-calculated from the equilibrium assumption. In practical applications, when heat loss is involved, T_b is smaller than 1720 K.

In order to satisfy the constraint $\sum_k^{N_{species}} x_k = 1$ during sampling, nitrogen is used as a passive species to absorb the uncertainty of the other dry species, *i.e.* $N_2^{dry} = 1 - H_2^{dry} - CO^{dry} - CO_2^{dry} - CH_4^{dry}$ for each sample. Hence the PDF support of N_2^{dry} will be $0.015 \times D = 0.06$. This introduces an error in Step 4, the Galerkin projection, because the flame quantity Q is now dependent on five dimensions rather than four. Previous studies have shown that the error is acceptable if the passive uncertainty is applied to species having little influence on the fluctuation of the flame quantity Q. In the present study, a stricter strategy is applied in that the passive species is forced to be an inert species except in three-body reactions. Thus, N_2^{dry} has very limited influence on the flame physico-chemical properties, except for being a heat absorber, and given its

relatively small uncertainty, its thermal effect can be considered negligible as well. This strategy, therefore, improves the accuracy of the UQ by reducing the perturbation from the passive uncertainty.

2.2. Main, joint, and deterministic sensitivity coefficient

The reason for building a PCE of the model output is the ease of obtaining sensitivity information (effect of the input variance on the output variance) from the PCE terms. The PCE of the output quantity Q, truncated at order P, can be written as:

$$Q(\lambda) \cong \sum_{i=0}^{P} C_i \psi_{\boldsymbol{\alpha}^i}(\boldsymbol{\xi}); \tag{3}$$

where C_i are the PC coefficients and $\psi_{\boldsymbol{\alpha}^i}(\boldsymbol{\xi})$ is the multivariate Legendre polynomial of degree i, defined as:

$$\psi_{\boldsymbol{\alpha}^i}(\boldsymbol{\xi}) = \prod_{k=1}^{D} \mathscr{L}_{\alpha_k^i}(\xi_k). \tag{4}$$

here, $\mathscr{L}_{\alpha_k^i}(\xi_k)$ is the univariate Legendre polynomial of degree α_k^i, function of ξ_k, and $\boldsymbol{\alpha}^i$ is the set of polynomial degrees whose sum is equal to the degree i :

$$\boldsymbol{\alpha}^i = \left\{ \alpha_k^i \geq 0 : \sum_{r=1}^{D} \alpha_r^i = i \right\} \tag{5}$$

It can be shown ([33]) that the variance of the PCE is:

$$Var[Q] \cong \sum_{i=0}^{P} C_i^2 E\left[\psi_{\boldsymbol{\alpha}^i}{}^2(\boldsymbol{\xi})\right] \tag{6}$$

Eq. (3) can be rearranged by gathering the terms according to their dependence on the input parameters:

$$\begin{aligned} Q \cong & f_0 + \sum_{i=1}^{D}\sum_{j=1}^{P} f_{\alpha_i^j} \psi_{\alpha_i^j}(\xi_i) + \sum_{i_1=1}^{D}\sum_{i_2=i_1+1}^{D} \\ & \times \sum_{j=1}^{P} f_{\left(\alpha_{i_1}^j, \alpha_{i_2}^j\right)} \psi_{\left(\alpha_{i_1}^j, \alpha_{i_2}^j\right)}(\xi_{i_1}, \xi_{i_2}) + \cdots + \sum_{i_1=1}^{D} \cdots \sum_{i_n=i_{n-1}+1}^{D} \\ & \times \sum_{j=1}^{P} f_{\left(\alpha_{i_1}^j, \cdots, \alpha_{i_n}^j\right)} \psi_{\left(\alpha_{i_1}^j, \cdots, \alpha_{i_n}^j\right)}(\xi_{i_1}, \cdots, \xi_{i_2}) + \cdots + \sum_{j=1}^{P} f_{\left(\alpha_1^j, \cdots, \alpha_D^j\right)} \psi_{\left(\alpha_1^j, \cdots, \alpha_D^j\right)}(\xi_1, \cdots, \xi_D) \end{aligned} \tag{7}$$

This form is identical to the Sobol decomposition of Q [27], and can be used to directly calculate the Sobol indices (or sensitivity indices), *i.e.*, the contributions of all possible subsets of input parameters to the total variance.

In the present work, we are interested in the *main sensitivity index*:

$$S_i = \frac{\sum_{k=1}^{P} f_{\alpha_i^k}{}^2 E\left[\psi_{\alpha_i^k}(\xi_i)^2\right]}{Var[Q]}; \tag{8}$$

i.e., the contribution of the input variable i on the total variance, when taken by itself, and the *joint sensitivity index*:

$$S_{ij} = \frac{\sum_{k=1}^{P} f_{\left(\alpha_i^k, \alpha_j^k\right)}{}^2 E\left[\psi_{\left(\alpha_i^k, \alpha_j^k\right)}(\xi_i, \xi_j)^2\right]}{Var[Q]}; \tag{9}$$

i.e., the contribution of the pair of input variables (i, j) when taken by itself.

While the main and joint sensitivity indices allow to evaluate the statistical effect of wet bio-syngas variability on the fluctuation of the flame physicochemical properties, it is difficult to assess how the steam addition may have changed the chemical pathways of individual species and altered the radical pools balance.

Therefore, a conventional (*i.e.*, deterministic) sensitivity study is also carried out, showing the sensitivity of the flame temperature to individual reactions when the steam content is changed. We define the deterministic sensitivity coefficient f_i as:

$$f_i = \frac{\partial lnQ}{\partial lnk_i} = \frac{k_i}{Q} \times \frac{\partial Q}{\partial k_i} \approx \frac{Q_{after} - Q_{before}}{Q_{before} * \Delta k_i}; \tag{10}$$

where Δk_i is a small perturbation applied to the rate constant of reaction i, and Q_{before} and Q_{after} is the flame property calculated before and after the perturbation Δk_i respectively.

Summarising, the main and joint sensitivity indices show the effect of fluctuations of the bio-syngas composition on the statistics of the flame properties, while the deterministic sensitivity coefficient shows the effect of steam content on the chemical reaction pathways of fixed bio-syngas composition.

2.3. Chemical mechanisms

Before proceeding to the UQ analysis, it is necessary to validate the existing reaction mechanisms in conditions of high H_2O content. To the knowledge of the authors, no skeletal mechanisms are specifically developed for ultra-wet bio-syngas combustion. However, several mechanisms which may be feasible in ultra-wet conditions can be validated in $CO/H_2/O_2/H_2O$ environment [13,34]. Though the validating cases do not involve CH_4 and N_2 reactions, most existing mechanisms for methane combustion in O_2/N_2 environment can be applied with little concern. It is the high H_2O content and its effect on the formation and consumption of H and OH radicals and on three-body reactions that require extra care.

In the present study, the mechanisms chosen for validation are: GRI Mech3.0 [35], SanDiego Mechanism [36], USC Mechanism [37], Davis Mechanism [38], and FFCM-1 [39]. Although the GRI Mech3.0 is widely used for C reactions, its performance in $CO/H_2/O_2/H_2O$ environment is doubtful. This also applies to the SanDiego Mechanism. The performance of the Davis mechanism was validated by Sun *et al.* [34], Meng *et al.* [13] in $CO/H_2/O_2/H_2O$ environment. Reasonable flame speed predictions were reported only when the H_2 content in the reactants is low. Since the Davis mechanism does not include CH_4 reactions, it is here considered only for comparison with the USC mechanism, and it is not included in the UQ analysis. The USC Mechanism refers to a high-temperature $H_2/CO/C_1$-C_4 reaction model optimized based on the Davis Mechanism, GRI Mech2.11, GRI Mech 3.0, *etc.*

In addition to the above widely used mechanisms, the FFCM-1, released in 2016 as an $H_2/CO/C_1$ reaction mechanism, invokes the UQ analysis to carry out forward propagation and backward minimization of rate coefficient uncertainties against experiment datasets for fuel/species sets H_2, CO, CH_2O, CH_4, H_2O_2, and C_2H_6. Although not optimized specifically for high steam content combustion, the mechanism shows great potential for such a purpose, as will be shown in Section 3.1. A recent report by Tao *et al.* [40] showed good performance of this mechanism under various combustion conditions, attributing to its employed UQ method to reduce reaction mechanism uncertainty. In fact, using UQ for reducing uncertainty in reaction mechanism was broadly discussed in many literatures [41,42], but using the method for investigating the effect of fuel variability, as given in the following sections, is still scarce.

3. Result and discussions

3.1. Validation of chemical mechanisms

Following the description of chemical mechanisms in Section 2.3, Fig. 1 shows a comparison of the predicted flame speed against experimental data [13] for CO/H_2 combustion in O_2/H_2O environment, with $Z_{H2O} = X_{H2O}/(X_{H2O} + X_{CO} + X_{H2} + X_{O2})$. The flame speed was experimentally measured at $\phi = 0.9$ and $T_u = 400$ K. All mechanisms agree

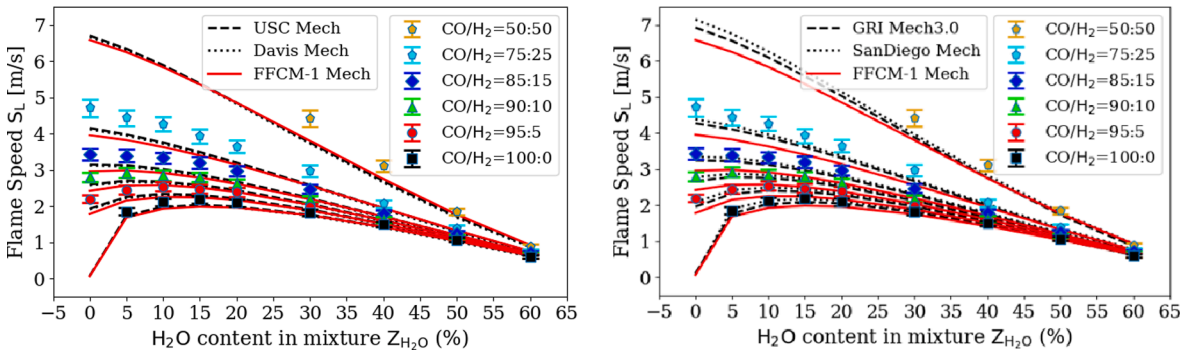

Fig. 1. Comparison between the experimental flame speed at $\phi = 0.9$ and $T_u = 400$ K [13] and different combustion mechanisms.

reasonably well with the experiment [13] and show roughly the same performance at $\phi = 0.9$. The best performing mechanism at this equivalence ratio is the SanDiego mechanism. Despite this fact, in Fig. 2, when experimental data [34] covers a wider range of equivalence ratios for $Z_{H2O} = 47\%$, the performance of the SanDiego mechanism deteriorates in the very rich combustion region. The GRI Mech3.0, USC and Davis mechanisms under-predict the flame speed when $CO/H_2 = 50:50$. The FFCM-1 mechanism has the best overall agreement over the entire equivalence ratios from 0.6 to 2.0; hence it is chosen for the UQ study in the following.

3.2. Uncertainty quantification of the flame physicochemical properties

3.2.1. Uncertainty effect on the flame temperature

The wet bio-syngas fuel variability effect on the adiabatic flame temperature T_{ad} is shown in Fig. 3. As discussed in Section 2.1, the estimated mean T_{ad} was fixed *a priori* around the value 1720 K, based on the nominal bio-syngas composition given in Table 1, by balancing $\{\phi, H_2O^{wet}\}$. The slight variation of mean T_{ad} in Fig. 3 (less than 10 K across the various cases) is due to the accuracy of this balancing calculation.

In Fig. 3, the mean $\mu_{T_{ad}}$ is the first mode of the PCE, *i.e.*, C_0 in Eq. (3), while the standard deviation $\sigma_{T_{ad}}$ is the square root of the variance directly evaluated from Eq. (6). The fluctuation T'_{ad} is defined as the coefficient of variation $(\mu_{T_{ad}}/\sigma_{T_{ad}})$. The fluctuation increases when ϕ increases from 0.6 to 1.0 and when CH_4^{dry} increases from 0.05 to 0.15. A maximum T'_{ad} of roughly 2% occurs for low LHV bio-syngas ($CH_4^{dry} = 0.05$) at stoichiometric condition, indicating that a thermal efficiency ($\eta = 1 - T_{in}/T_{ad}$) may vary from 51.6% to 56.7%, corresponding to a minimum $T_{ad} \approx 1610K$ and a maximum $T_{ad} \approx 1800K$, as shown in Fig. 4. The PDFs of Fig. 4 are obtained from 1,000,000 flame temperature evaluations using the PCE.

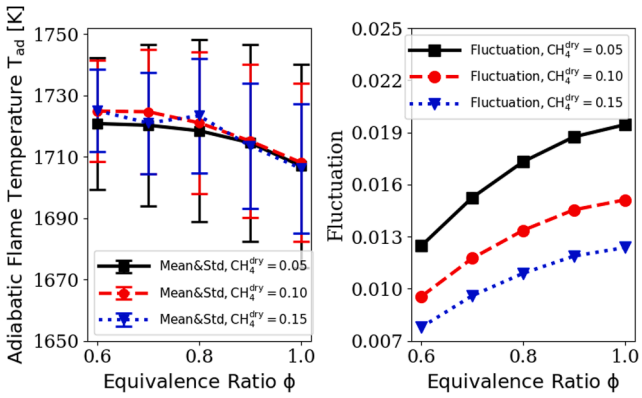

Fig. 3. Mean, standard deviation and fluctuation of T_{ad}.

Fig. 5 shows the four main sensitivity indices. It is noticed that the impact of the bio-syngas composition variability on T'_{ad} follows the order $S_{CH4} > S_{CO} > S_{H2} > S_{CO2}$. When CH_4^{dry} increases, this order remains unchanged. When $\phi = 1$, the variance of methane alone is responsible for nearly 80% of the total variance of T_{ad}. This indicates that, for an HGT running on bio-syngas, feedstock from that produces methane after gasification needs extra care. For example, if wood chips are the feedstock responsible for the CH_4 content in a batch of bio-syngas, one may want to ensure that these wood chips are produced in a consistent shape, contain the same moisture content, and are stored at the same conditions before being used. Other than the feedstock issue, stable CH_4 content also depends on stable control of the steam-reforming process during the gasification operation.

Besides, in Fig. 5, it can be seen that the methane uncertainty effect

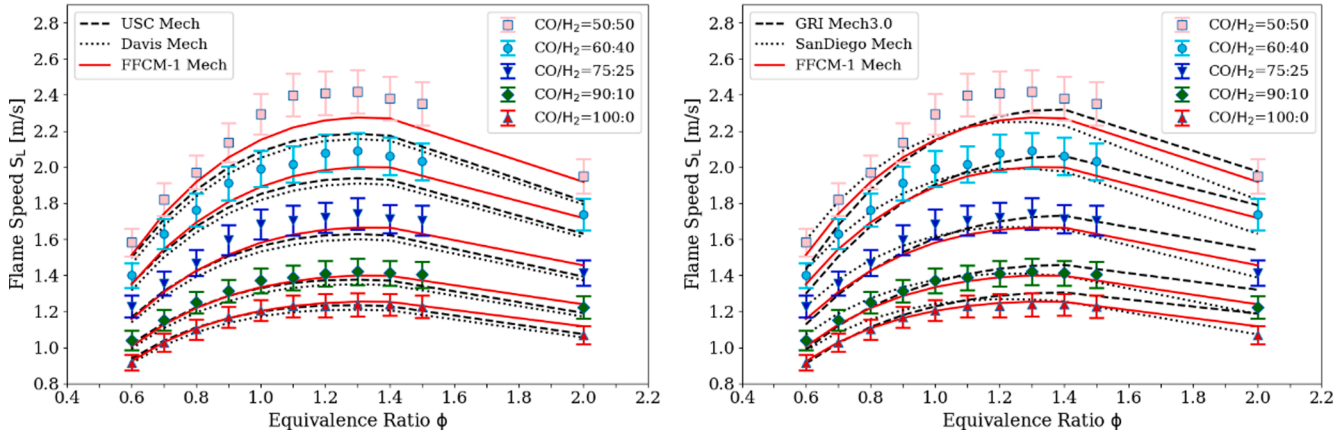

Fig. 2. Comparison between the experimental flame speed at $Z_{H2O} = 47\%$ and $T_u = 400$ K [34] and different combustion mechanisms.

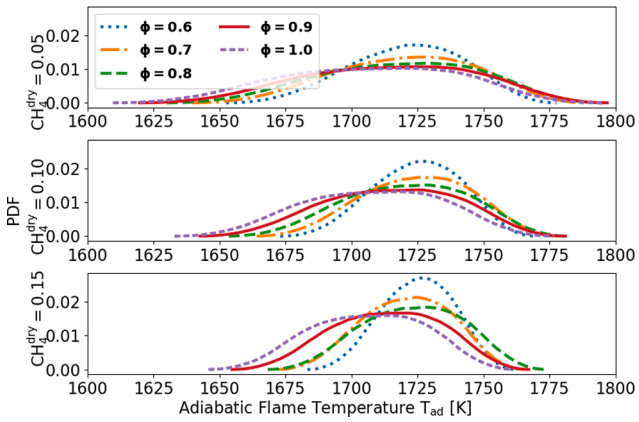

Fig. 4. PDFs of T_{ad} for different ϕ and CH_4^{dry}.

on the flame temperature is influenced by $\{\phi, H_2O^{wet}\}$. Note that each ϕ in the legend is associated with a different H_2O^{wet} with values given in Table 1. When $\{\phi, H_2O^{wet}\}$ increases, the sensitivity of the flame temperature variance to the methane variance also increases, in association with a reduction of the temperature sensitivity to the hydrogen variance. The large methane contribution to the flame temperature variation was never reported in previous literature, though different fuels were analysed. In contrast, hydrogen uncertainty was deemed to have the largest impact on the flame temperature variation. It is speculated that the high impact of methane in the present study is due to the high steam content in the bio-syngas, which influences subsequent chemical pathways. This new finding is of great importance to run HGT using wet fuel with large composition variability.

To illustrate the impact of steam content on chemical pathways, a sensitivity analysis is performed in the post-combustion region ($\sim 1ms$ after flame front) where T_{ad} is chosen for building PCEs. The deterministic sensitivity coefficient of T_{ad} for case 1: CH_4^{dry}=0.05 is shown in Fig. 6. The ten most sensitive reactions relevant to the three species of interest, CH_4, H_2, and H_2O, are shown. For the convenience of comparison, x-axes are labeled with the same range, even though this sometimes leads to a difficult visualization of the reactions with low sensitivity indices.

Comparing Fig. 6a and 6b, it is apparent that the CH_4 reactions are more sensitive to the change of $\{\phi, H_2O^{wet}\}$ compared to the H_2 reactions, though some reactions are shared by the two species. Out of the three species, H_2O has the most rapidly increasing impact on the change of T_{ad} when $\{\phi, H_2O^{wet}\}$ increases. This is mainly attributed to the promoted forward reactions R14: $2H_2O = H + H_2O + OH$ and R13: $H_2O + M = H + OH + M$, which produce H and OH radicals via H_2O dissociation. Although the H radical limits CH_4 dissociation via R97: $CH_3 + H = CH_4$, the OH radical promotes the hydrogen abstraction reaction R138: $CH_4 + OH = CH_3 + H_2O$ [43], to partially favour the higher impact of the CH_4 uncertainty on $T_{ad}^{'}$. The promoted forward reaction R136: $CH_4 + H = CH_3 + H_2$ also plays the same role at high $\{\phi, H_2O^{wet}\}$, meanwhile reducing the contribution of H_2 to the adiabatic flame temperature together with R16: $H + HO_2 = H_2 + O_2$. From a chemical perspective, the parameter variability in the third body dissociation reactions featuring H_2O may introduce extra uncertainties to the UQ analyses. This issue will be investigated by the authors in the future UQ studies, while it is out of the scope of the present work focusing on the uncertainties introduced by fuel variabilities in a macroscale.

3.2.2. *Uncertainty effect on the flame speed and flame thickness*

Variations of the laminar flame speed S_L and the flame thickness δ_L due to fuel variability can greatly change combustion/flame behaviour, which may lead to flame blow-off, flashback, and thermo-acoustic instability. In the sense of combustion modelling, although it was shown that the commonly employed scaling method fails, alternative formulations can still work surprisingly well [44,45]. While these studies do not consider wet mixtures, forward pushing the established uncertainty effect in the present work through similar formulations (*e.g.* by varying Zimont turbulent flame speed closure method [46,47]) results in modelling approaches capable of predicting quantified safety margins. High Karlovitz (*Ka*) and high Reynolds (*Re*) number flames stabilised with swirling flow, as often found in an industrial humidified gas turbine (HGT), are particularly sensitive to the issue.

Fig. 7 shows the impact of the wet bio-syngas fuel variability on S_L and δ_L. As was the case for T_{ad} in Fig. 4, uniformly distributed wet bio-syngas composition uncertainties lead to bell-shaped distributions of S_L and δ_L. It is observed that the variance of the flame speed has negligible dependence on the change of $\{\phi, H_2O^{wet}\}$, while the variance of the flame thickness is very sensitive to it. For instance, at a fixedCH_4^{dry} = 0.05, increase ϕ (and hence equivalent to increase $\{\phi, H_2O^{wet}\}$) does not change the variance of S_L - the change of S_L is always ~30 cm/s, while it increases the variance of δ_L - the change of δ_L amplifies from ~0.18 mm to ~0.4 mm. When methane content in dry bio-syngas increases, mean flame speed decreases and flame thickness increases due to less highly reactive and diffusive H_2 and H radicals in reactants. The same observation can also be identified in Fig. 8 with mean S_L and its fluctuation S_L' explicitly plotted. In Fig. 8, the standard deviation of S_L decreases while the standard deviation of δ_L increases with increased methane content in dry bio-syngas.

In terms of fluctuation, S_L' and $\delta_L^{'}$ follows roughly the same trend that they both increase at higher content of CH_4^{dry} or $\{\phi, H_2O^{wet}\}$. The impact of $\{\phi, H_2O^{wet}\}$ on S_L' and $\delta_L^{'}$ is seen much larger than that of CH_4^{dry}. For instance, at a fixed $\phi = 0.6$, increase CH_4^{dry} from 0.05 to 0.15 has little impact on S_L' and $\delta_L^{'}$; while at a fixed CH_4^{dry}, increase ϕ from 0.6 to 1.0 significantly modifies the two quantities. The highest fluctuation of S_L and δ_L are observed to be nearly 10% and 7.5% respectively at stoichiometric condition, a case of highly steam-diluted bio-syngas. Note that for an HGT running on highly steam-diluted bio-syngas with $CH_4^{dry} = 0.15$ and $\phi = 1$, occasional changes of flame speed and flame

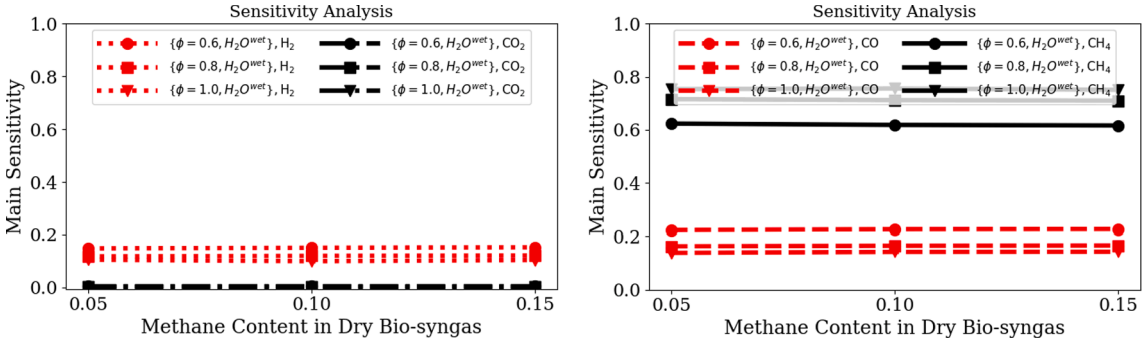

Fig. 5. Main sensitivity indices relative to the adiabatic flame temperature. Each ϕ in the legend is associated with a different H_2O^{wet} at a typical methane content.

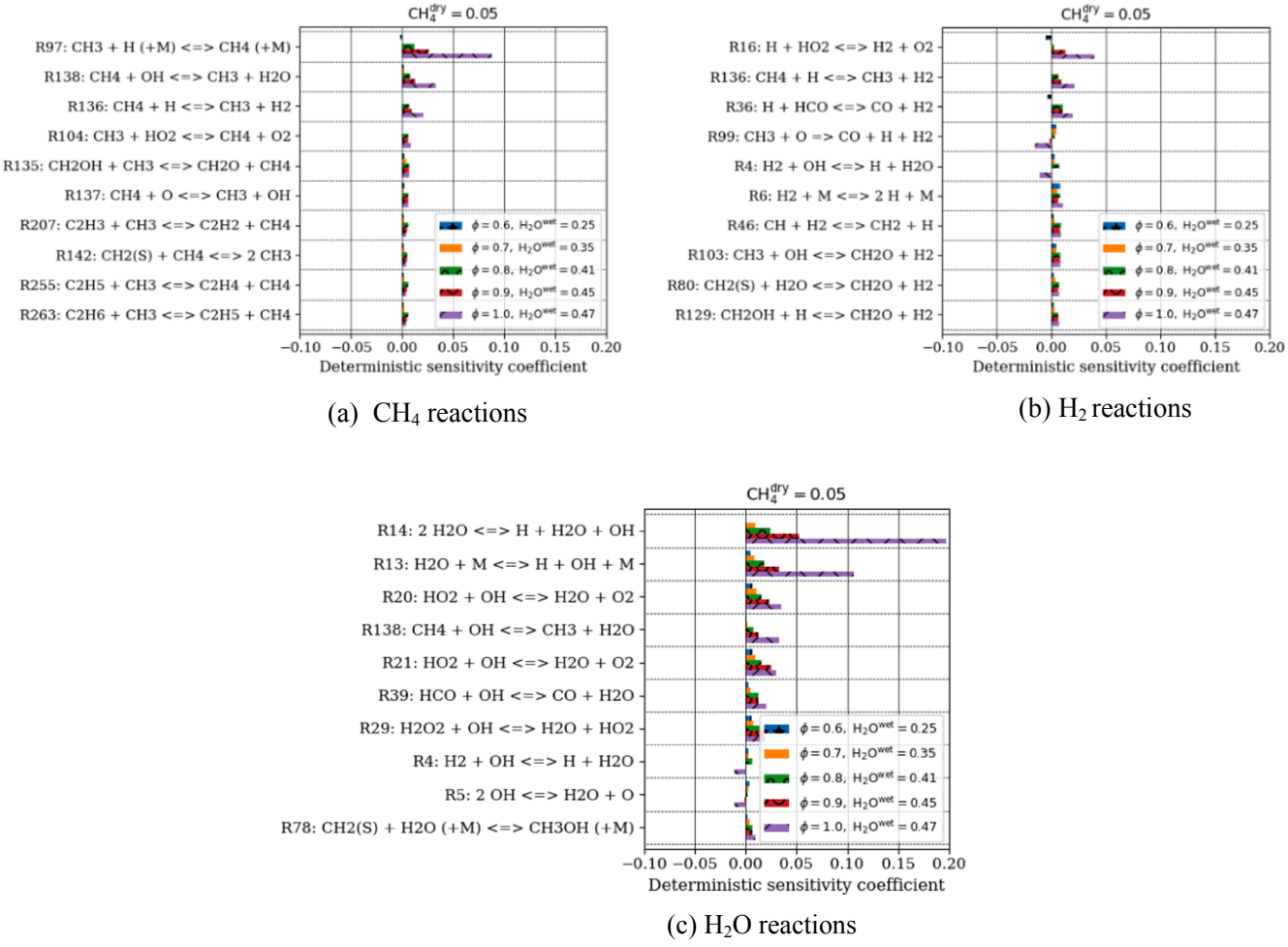

(a) CH_4 reactions (b) H_2 reactions

(c) H_2O reactions

Fig. 6. Deterministic sensitivity coefficient of T_{ad} to chemical reactions.

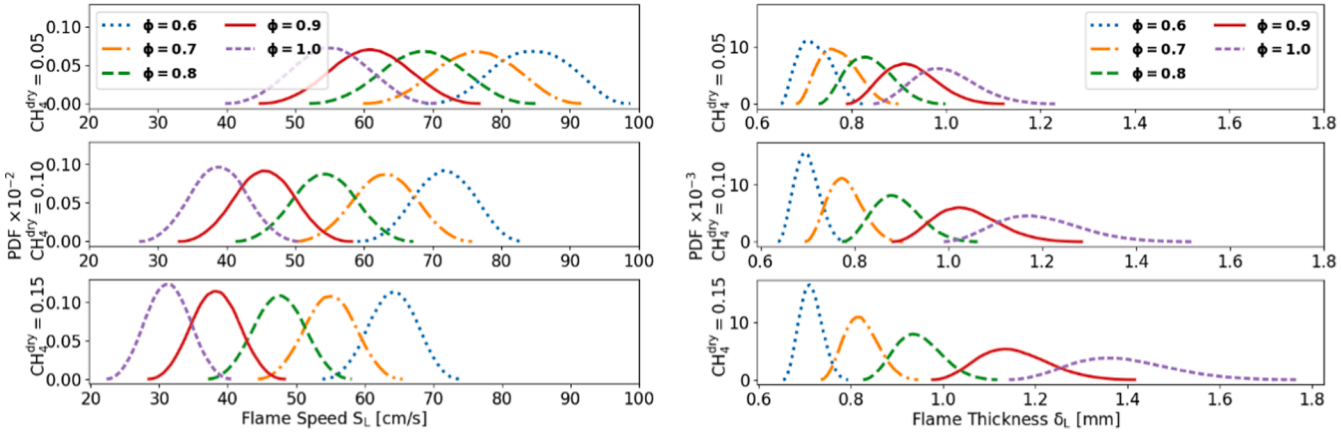

(a) Flame Speed S_L (b) Flame thickness δ_L

Fig. 7. PDFs of S_L for different ϕ and CH_4^{dry}. Each ϕ in the legend is associated with a different H_2O^{wet} at a typical methane content.

thickness may lead to serious operational failure.

For instance, consider the small-scale 60 KW HP burner developed at TU berlin [11,48,49] running on wet bio-syngas. Table 2 shows the flame properties, Reynolds number (Re) and Karlovitz number (Ka) for the three points labelled in Fig. 9. This figure shows the PDF of the flame speed for case 3 at stoichiometric conditions, extracted from Fig. 7. The Reynolds number and Karlovitz number are two key factors influencing flame stabilisation, together with the swirl number.

To calculate $Re = U_{bulk}L/\nu$, the characteristic length L is chosen to be the mixing tube diameter of the HP burner: $D_m = 0.034$ m. The bulk velocity (U_{bulk}) is calculated based on a constant thermal power of 60KW, the LHV of the bio-syngas compositions corresponding to the three points in Fig. 9, and the mixing tube cross-section. The Karlovitz number is defined as,

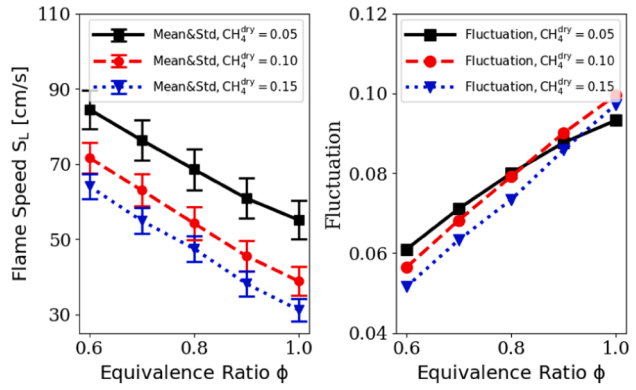

(a) Flame Speed S_L

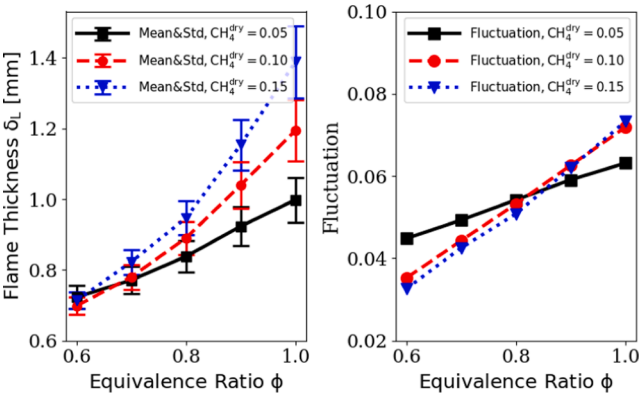

(b) Flame thickness δ_L

Fig. 8. Mean, standard deviation and fluctuation of S_L and δ_L.

$$Ka \sim \left(\frac{u'}{S_L}\right)^{1.5}\left(\frac{\delta_L}{D_m}\right)^{0.5}; \quad (8)$$

where velocity fluctuation $u' = 15\%U_{bulk}$ in the burner is widely used to calculate global *Ka*. From Table 2, *Ka* increases by three times when the bio-syngas composition changes from the high LHV to the low LHV point. In the meantime, *Re* is reduced by 14000, roughly 10%. Although a flame with these dimensionless values is most likely still in the thin reaction zone (Borghi diagram [50,51]), the percentage change of *Ka* and *Re* for a practical HGT (which is upscaled by a factor of about 1000 in terms of power output) will result in serious operating issues, which is risky even if the probability of occurrence for the high and low points in Fig. 9 is very low.

The sensitivity indices identify which species in the bio-syngas are responsible for the above large fluctuations. In Fig. 10, it is seen that when CH_4^{dry} is low, the variance of flame speed is dominated by the species uncertainty in the following order: $S_{H2} > S_{CO} > S_{CH4} > S_{CO2}$. For higher CH_4^{dry}, the contribution of methane to S_L' increases and that of hydrogen decreases, while the sensitivity to the other species does not change much. The sensitivity order of species variability on $\dot{\delta_L}$ follows $S_{CH4} > S_{H2} > S_{CO} > S_{CO2}$ and the order is less affected by mean methane content in dry bio-syngas compared to the flame speed.

The joint role of CH_4 and H_2 on S_L' and $\dot{\delta_L}$ is confirmed by the joint sensitivity study shown in Fig. 11. Only the result for the case with $CH_4^{dry} = 0.05$ is shown, as the other two cases show essentially the same trend. The joint sensitivity indices involving CO_2 always have little contribution to the flame speed variation, as CO_2 contributes scarcely to the reactions of the other species, and mainly acts as a heat source being produced by combustion. The S_{H_2,CH_4} index always gives the highest contribution to the fluctuation of S_L and δ_L, and is strongly influenced by $\{\phi, H_2O^{wet}\}$.

3.2.3. Uncertainty effect on the CO emissions

In addition to the impact of fuel variability on T_{ad}, S_L and δ_L, CO emissions are of great concern for an HGT running on wet bio-syngas. This is driven by two mechanisms: first, a flame that is unstable due to fuel variability can produce high CO emissions owing to local incomplete combustion; second, ultra-wet combustion in an HGT cycle often needs a high equivalence ratio far from the lean blow-out (LBO) limit in order to sustain the flame, which in turn leads to higher CO emissions. Moreover, it is reported that the CO emissions from wet combustion are strongly affected by the CO oxidation by OH (from decomposed H_2O) in the downstream flue gas pathway, and are hence highly influenced by the flue gas temperature and residence time [11,52]. In the vicinity of the flame, however, the CO production increases with increasing steam dilution, when the adiabatic flame temperature is fixed by varying $\{\phi, H_2O^{wet}\}$. One efficient way to reduce CO emissions is to elevate the HGT operating pressure, which is often the case in practical HGT industrial operation.

Fig. 12 shows the effect of the wet bio-syngas variability on the flue gas CO content. Note that the unit of CO emissions, 'ppmvd', is defined as volumetric parts per million on the dry bio-syngas base, same as it is often used in experimental measurements. A rapid increase in CO emissions occur when ϕ increases from 0.9 to 1.0. The inhibiting effect of the increased H_2O content on the CO production is outbalanced by the increased equivalence ratio which promotes CO formation. The highest CO emission fluctuation of 23% occurs when the equivalence ratio is 0.8 and $CH_4^{dry} = 0.05$, and the lowest fluctuation of 10% occurs at stoichiometric conditions. These fluctuations are induced by fuel variability only, but in real flames, when the fuel variability leads to flame instability, fluctuation magnifies.

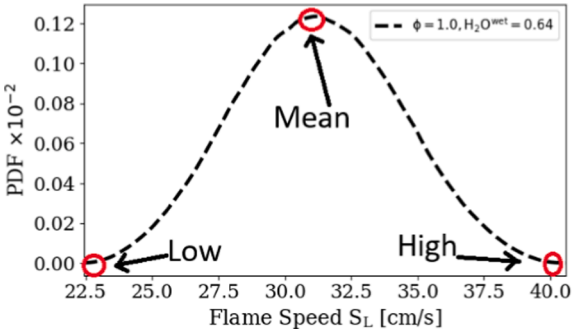

Fig. 9. PDF of S_L for case 3 at $\{\phi = 1.0, H_2O^{wet} = 0.64\}$.

Table 2
Bio-syngas composition and flame properties relative to the three points of Fig. 9.

Case 3	Dry Bio-syngas Gas Composition					S_L (cm/s)	δ_L (mm)	LHV (MJ/Kg)	*Re*	*Ka*
	H_2^{dry}	CO^{dry}	CO_2^{dry}	CH_4^{dry}	N_2^{dry}					
High	0.089	0.154	0.165	0.165	0.427	40.46	1.11	7.483	113,000	11.60
Mean	0.074	0.140	0.179	0.150	0.457	30.11	1.38	6.55	105,000	20.14
Low	0.060	0.125	0.190	0.135	0.490	22.32	1.77	5.670	99,000	32.69

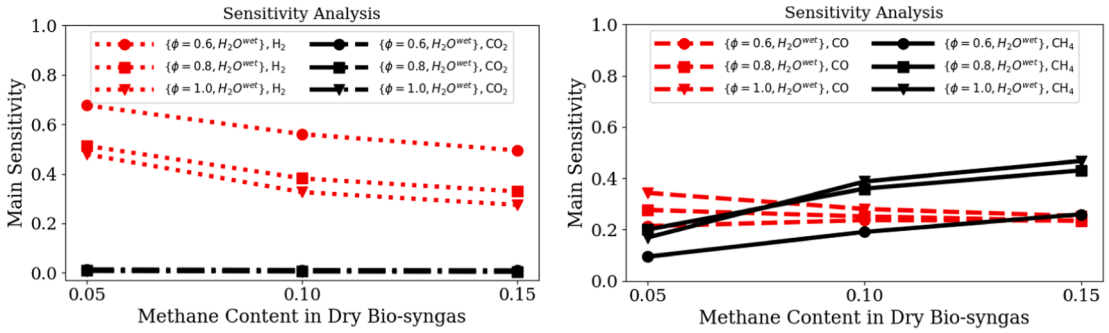

(a) Flame speed S_L

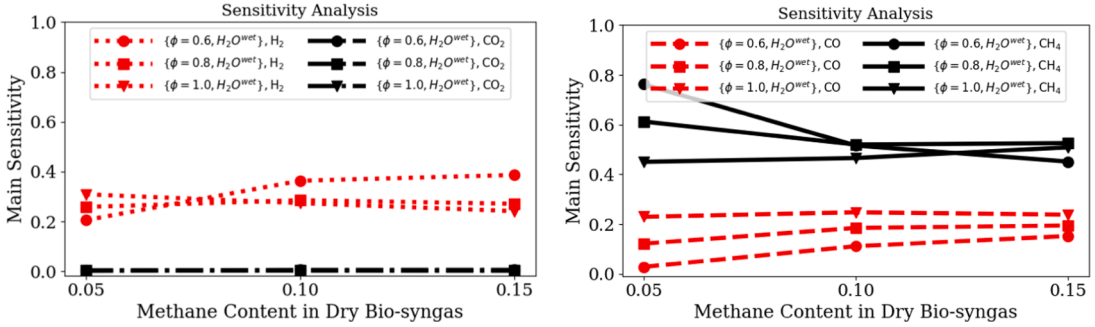

(b) Flame thickness δ_L

Fig. 10. Main sensitivity indices relative to the flame speed and the flame thickness. Each ϕ in the legend is associated with a different H_2O^{wet} at a typical methane content.

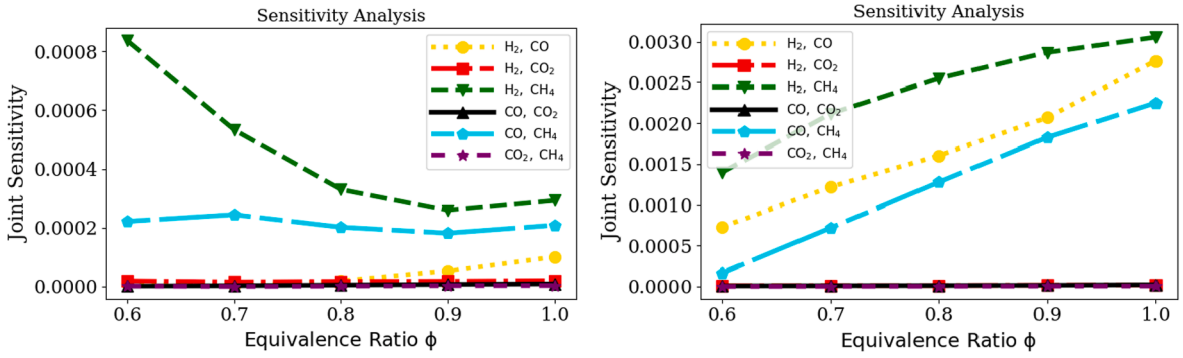

Fig 11. Joint sensitivity indices relative to the flame speed (left panel) and flame thickness (right panel) for$CH_4^{dry} = 0.05$.

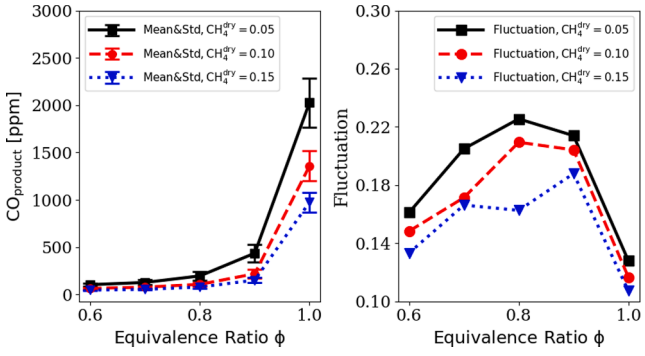

Fig. 12. Mean, standard deviation and fluctuation of CO emissions.

The mean CO values in Fig. 12 are much larger than often reported because a 1D premixed calculation presents the highest possible CO emission at the highest flame temperature. In real burners or combustors, the position of the high CO value reported in Fig. 12 locates at where the highest OH intensity is observed.

To obtain a practical mean CO emission value, a plug flow reactor (PFR) is built using Cantera [22] to post-process the CO emissions given in Fig. 12. The inlet velocity of the PFR is set to 10 m/s, corresponding to the velocity in the post-flame region of the HP burner developed at TU Berlin. The exhaust tube of the TU Berlin burner extends for a length of roughly 1 m downstream of the main flame position, and the exhaust gas temperature for wet bio-syngas combustion is about 800 K. Following these parameters, the PFR length is reproduced by a sequence of 2000 perfectly stirred reactors (PSR), each with a fixed rate of convective heat transfer to the environmental temperature of 300 K. This ensures that the outlet temperature of the last PSR is approximately 800 K. After post-processing, the CO emission drops to a much lower value, as seen in

Fig. 13. The first PSR is fed with a flame temperature of 1720 K and the same CO concentration shown in Fig. 12. As the CO proceeds downstream, it is oxidised by the OH radical, which is more abundant than oxygen. Except for $\phi = 1.0$, the CO level drops below 10 ppm when the exhaust gas temperature is lower than 1150 K. A higher CO level is observed for higher $\{\phi, H_2O^{wet}\}$, indicating a prominent effect of the equivalence ratio on increasing CO emissions over the CO suppression effect of steam dilution. Moreover, although the final exhaust gas temperature is often much lower than 800 K in a practical HGT cycle, no apparent CO decrease may be observed for temperatures lower than around 900 K. Cleaner combustion in terms of CO emissions can be achieved for bio-syngas containing more methane.

For consistency, the high CO emission level shown in Fig. 12 is used for sensitivity analysis. The results, shown in Fig. 14, reveal that the variance of the CO emissions is dominated by the wet bio-syngas composition variability following the order $S_{CH4} > S_{CO} > S_{H2} > S_{CO2}$. The methane index is above 50% in most cases. This sensitivity order is the same as that of temperature given in Fig. 5, and the CH_4^{dry} content in the bio-syngas has little impact on changing the sensitivity order. These results are expected, as the adiabatic flame temperature reflects the reaction progress in a 1D premixed flame simulation, and the reaction progress is directly related to the CO emissions for incomplete combustion.

4. Conclusions

The effect of steam-diluted bio-syngas composition variability on flame physicochemical properties is investigated employing a PCE based UQ method. The accuracy of the method is improved by prohibiting species containing passive uncertainty to interact with other species. A constant adiabatic flame temperature (T_{ad}) is pre-calculated by co-varying the equivalence ratio and the steam content $\{\phi, H_2O^{wet}\}$. This ensures that the sensitivity study is not influenced by temperature variation due to varying equivalence ratio. In a practical HGT cycle, an adiabatic flame temperature lower than 1720 K is required to avoid downstream turbine damage and to retain constant thermal efficiency. The variation of T_{ad} around 1720 K at a typical $\{\phi, H_2O^{wet}\}$ can only be a result of the fuel composition variability.

Several reaction mechanisms, the GRI Mech3.0, SanDiego Mechanism, USC Mechanism, Davis Mechanism, and FFCM-1, are validated against experimental flame speed data of highly steam-diluted CO/H_2 in an O_2 environment. The FFCM-1 mechanism has the best overall agreement over the entire tested equivalence ratios; hence it is recognized as an accurate mechanism to predict flame physicochemical properties for steam-diluted bio-syngas.

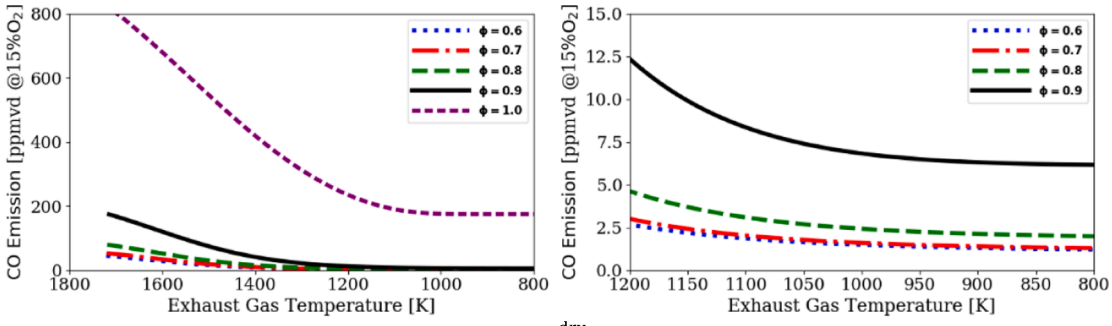

(a) CH_4^{dry}=0.05

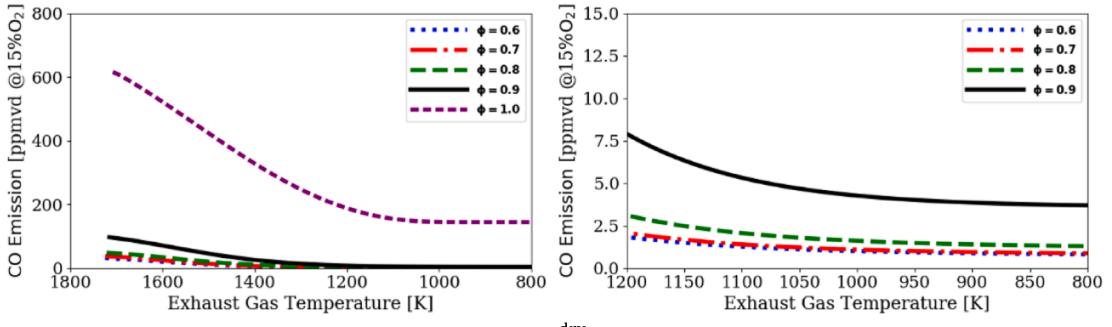

(b) CH_4^{dry}=0.10

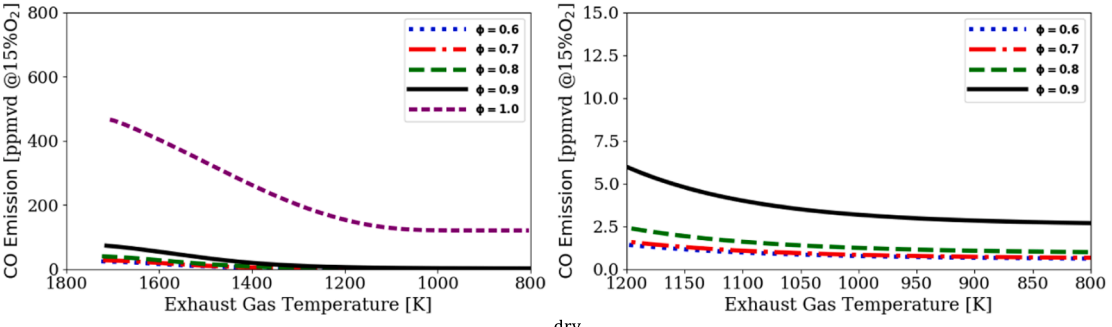

(c) CH_4^{dry}=0.15

Fig. 13. Post-processed CO emission level using 2000 sequential perfectly stirred reactors (right panels are zoom-in of the left).

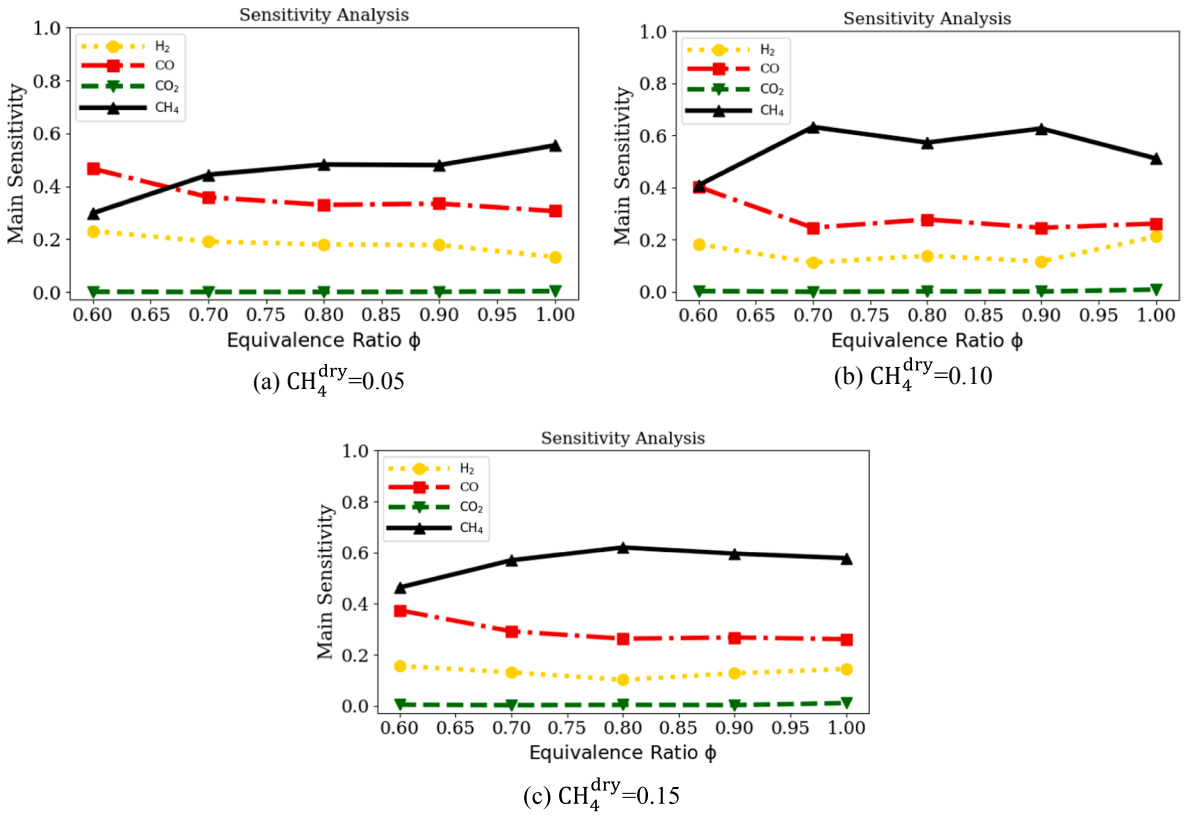

Fig. 14. Main sensitivity indices relative to the CO emission.

Assuming a uniformly distributed PDF with a small variance of 0.75% for the mole fraction of the bio-syngas composition, bell-shaped PDFs of T_{ad} and S_L are observed. Defining the fluctuation of a flame quantity as its coefficient of variation (ratio of the standard deviation to mean), a maximum 2% fluctuation of T_{ad} is observed at $\phi = 1.0$ for methane content in dry bio-syngas equal to 5%. Lower $\{\phi, H_2O^{wet}\}$ or less methane content in the dry bio-syngas reduce T_{ad}'. The main sensitivity indices show that 80% of the fluctuation is dominated by the uncertainty of CH_4, followed by CO, H_2, and CO_2. This order is different from the one previously reported in the literature, due to the promoted reaction rate of R14: $2H_2O = H + H_2O + OH$ and R13: $H_2O + M = H + OH + M$ in a wet environment, which favours the reaction of methane but inhibits the reaction of hydrogen. Due to the small 2% fluctuation of adiabatic flame temperature, the thermal efficiency of an HP burner can vary from 51.6% to 56.7%.

The flame speed and flame thickness, which are vital factors influencing the flame stability and combustion regime, are very sensitive to wet bio-syngas variability. A maximum S_L' of 10% and δ_L' of 7.5% are observed at stoichiometric conditions. The dry methane mole fraction in the bio-syngas has limited influence on these fluctuations, while they are very sensitive to the change of $\{\phi, H_2O^{wet}\}$. The importance of these observations is highlighted by the calculation of *Ka* and *Re* using the parameters of an HP burner, developed at TU Berlin, Germany, for $CH_4^{dry} = 0.15$. An absolute change of *Ka* by 20 (300% by fraction) and *Re* by 14,000 (10% by fraction), due to the fuel variability, can have a serious impact on practical flame stability. The main sensitive indices show that the variance of hydrogen dominates the flame speed fluctuation, while the variance of methane dominates the flame thickness fluctuation. It is reported for the first time that the largest fluctuation of CO is observed at an equivalence ratio of 0.8, and is dominated by uncertainty of methane content in the fuel. Co-increasing the equivalence ratio and steam content to keep a constant flame temperature is seen to increase the CO emissions.

Overall, the present study provides new findings on how an HGT running on steam diluted bio-syngas may experience flame instability due to fuel variability. Guidance on practical application of the HGT technology is provided that a) an HGT cycle is cleaner by burning wet bio-syngas containing high methane content, while this leads to less stable combustion and less stable thermal efficiency from a view of fuel variability; b) although the HGT technology with more steam content involved in combustion process is known more electrical efficient compared to the traditional thermal power plants, it suffers from stronger combustion instability compared to dry combustion. This is a result of not only the lower reactivity of diluted wet bio-syngas but also the fuel composition variability, especially the methane variability. Guarantee the stable methane production, during the upstream gasification process to produce bio-syngas, is a key to ensure safe and stable operation of the HGT cycle.

Further studies are being performed by the authors to investigate high-pressure impact on the stable operation of HGT, which is of practical relevance to industrial renewable energy production.

CRediT authorship contribution statement

Kai Zhang: Methodology, Formal analysis, Investigation, Writing - original draft. **Giandomenico Lupo:** Writing - review & editing. **Christophe Duwig:** Conceptualization, Writing - review & editing, Supervision, Funding acquisition.

Declaration of Competing Interest

The authors declare that they have no known competing financial interests or personal relationships that could have appeared to influence the work reported in this paper.

Acknowledgements

The financial support of Phoenix BioPower AB is greatly acknowledged.

The computations were performed on resources provided by the Swedish National Infrastructure for Computing (SNIC) on LUNARC and PDC.

References

[1] Rydstrand MC, Westermark MO, Bartlett MA. An analysis of the efficiency and economy of humidified gas turbines in district heating applications. Energy 2004; 29(12–15):1945–61.
[2] Jonsson M, Yan J. Humidified gas turbines—a review of proposed and implemented cycles. Energy 2005;30(7):1013–78.
[3] De Paepe W, Carrerro MM, Bram S, Parente A, Contino F. Advanced humidified gas turbine cycle concepts applied to micro gas turbine applications for optimal waste heat recovery. Energy Procedia 2017;105:1712–8.
[4] Carrero MM, De Paepe W, Bram S, Musin F, Parente A, Contino F. Humidified micro gas turbines for domestic users: An economic and primary energy savings analysis. Energy 2016;117:429–38.
[5] Phoenix Biopower. The BTC Technology — Phoenix Biopower; 2019. [online] Available at: https://phoenixbiopower.com/projects [Accessed 10 Nov. 2019].
[6] Casleton KH, Breault RW, Richards GA. System issues and tradeoffs associated with syngas production and combustion. Combust Sci Technol 2008;180(6):1013–52.
[7] Tumuluru JS, Wright CT, Boardman RD, Yancey NA, Sokhansanj S. A review on biomass classification and composition, co-firing issues and pretreatment methods. In: In 2011 Louisville, Kentucky, August 7-10, 2011. American Society of Agricultural and Biological Engineers; 2011. p. 1.
[8] Huang F, Jin S. Investigation of biomass (pine wood) gasification: Experiments and Aspen Plus simulation. Energy Science & Engineering; 2019.
[9] Cifuentes L, Fooladgar E, Duwig C. Chemical explosive mode analysis for a jet-in-hot-coflow burner operating in MILD combustion. Fuel 2018;232:712–23.
[10] Stathopoulos P, Kuhn P, Wendler J, Tanneberger T, Terhaar S, Paschereit CO, et al. Emissions of a wet premixed flame of natural gas and a mixture with hydrogen at high pressure. J Eng Gas Turbines Power 2017;139(4):041507.
[11] Kuhn, P., Terhaar, S., Reichel, T. and Paschereit, C.O., 2015, June. Design and Assessment of a Fuel-Flexible Low Emission Combustor for Dry and Steam-Diluted Conditions. In ASME Turbo Expo 2015: Turbine Technical Conference and Exposition. American Society of Mechanical Engineers Digital Collection.
[12] Stathopoulos, P., Terhaar, S. and Paschereit, C., 2014. The Ultra-Wet Cycle for High Efficiency, Low Emission Gas Turbines. In 7th International Gas Turbine Conference (ETN: IGTC-14), Brussels, Belgium, Oct (pp. 14-15).
[13] Meng S, Sun S, Xu H, Guo Y, Feng D, Zhao Y, et al. The effects of water addition on the laminar flame speeds of $CO/H_2/O_2/H_2O$ mixtures. Int J Hydrogen Energy 2016;41(25):10976–85.
[14] Xu H, Sun S, Liu F, Zhao Y, Liu Y, Chen L, et al. An experimental and computational study of OH formation in laminar coflow syngas diffusion flames. Fuel 2018;225: 47–53.
[15] Krejci MC, Keesee CL, Vissotski AJ, Ravi S, Petersen EL. Effect of steam dilution on laminar flame speeds of syngas fuel blends at elevated pressures and temperatures. ASME Turbo Expo 2019: Turbomachinery Technical Conference and Exposition. American Society of Mechanical Engineers Digital Collection. 2012.
[16] Nikolaou ZM, Chen JY, Swaminathan N. A 5-step reduced mechanism for combustion of $CO/H_2/H_2O/CH_4/CO_2$ mixtures with low hydrogen/methane and high H_2O content. Combust Flame 2013;160(1):56–75.
[17] Stylianidis N, Azimov U, Birkett M. Investigation of the effect of hydrogen and methane on combustion of multicomponent syngas mixtures using a constructed reduced chemical kinetics mechanism. Energies 2019;12(12):2442.
[18] Michael JV, Su MC, Sutherland JW, Carroll JJ, Wagner AF. Rate constants for $H+O_2+M \rightarrow HO_2+M$ in seven bath gases. J Phys Chem A 2002;106(21):5297–313.
[19] Lee HC, Jiang LY, Mohamad AA. A review on the laminar flame speed and ignition delay time of Syngas mixtures. Int J Hydrogen Energy 2014;39(2):1105–21.
[20] Zhang K, Jiang X. An investigation of fuel variability effect on bio-syngas combustion using uncertainty quantification. Fuel 2018;220:283–95.
[21] Zhang K, Jiang X. Uncertainty quantification of fuel variability effects on high hydrogen content syngas combustion. Fuel 2019;257:116111.
[22] David G. Goodwin, Raymond L. Speth, Harry K. Moffat, and Bryan W. Weber., 2018. Cantera: An object-oriented software toolkit for chemical kinetics, thermodynamics, and transport processes. https://www.cantera.org, Version 2.4.0. doi:10.5281/zenodo.1174508.
[23] Wiener N. The homogeneous chaos. Am J Mathe 1938;60(4):897–936.
[24] Wang H, Sheen DA. Combustion kinetic model uncertainty quantification, propagation and minimization. Prog Energy Combust Sci 2015;47:1–31.
[25] Reagan MT, Najm HN, Ghanem RG, Knio OM. Uncertainty quantification in reacting-flow simulations through non-intrusive spectral projection. Combust Flame 2003;132(3):545–55.
[26] Reagan MT, Najm HN, Pebay PP, Knio OM, Ghanem RG. Quantifying uncertainty in chemical systems modeling. Int J Chem Kinet 2005;37(6):368–82.
[27] Sobol IM. Sensitivity estimates for nonlinear mathematical models. Math Model Comput Experim 1993;1(4):407–14.
[28] Tomlin AS. The role of sensitivity and uncertainty analysis in combustion modelling. Proc Combust Inst 2013;34(1):159–76.
[29] Sobol' IYM. On sensitivity estimation for nonlinear mathematical models. Matematicheskoe modelirovanie 1990;2(1):112–8.
[30] Loh WL. On Latin hypercube sampling. Ann Stat 1996;24(5):2058–80.
[31] Davis PJ, Rabinowitz P. Methods of numerical integration. Courier Corporation; 2007.
[32] Basu P. Biomass gasification, pyrolysis and torrefaction: practical design and theory. Academic Press; 2018.
[33] Sudret B. Global sensitivity analysis using polynomial chaos expansions. Reliab Eng Syst Saf 2008;93(7):964–79.
[34] Sun S, Meng S, Zhao Y, Xu H, Guo Y, Qin Y. Experimental and theoretical studies of laminar flame speed of CO/H_2 in O_2/H_2O atmosphere. Int J Hydrogen Energy 2016;41(4):3272–83.
[35] Smith GP, Golden DM, Frenklach M, Moriarty NW, Eiteneer B, Goldenberg M, et al. GRI Mech 3.0, http://www.me.berkeley. edu/gri_mech/; 2006.
[36] Chemical-Kinetic Mechanisms for Combustion Applications", San Diego Mechanism web page, Mechanical and Aerospace Engineering (Combustion Research), University of California at San Diego (http://combustion.ucsd.edu).
[37] Hai Wang, Xiaoqing You, Ameya V. Joshi, Scott G. Davis, Alexander Laskin, Fokion Egolfopoulos, and Chung K. Law, USC Mech Version II. High-Temperature Combustion Reaction Model of H2/CO/C1-C4 Compounds.
[38] Davis SG, Joshi AV, Wang H, Egolfopoulos F. An optimized kinetic model of H_2/CO combustion. Proc Combust Inst 2005;30(1):1283–92.
[39] G. P. Smith, Y. Tao, and H. Wang, Foundational Fuel Chemistry Model Version 1.0 (FFCM-1), http://web.stanford.edu/group/haiwanglab/FFCM-1/index.html, 2016.
[40] Tao Y, Smith GP, Wang H. Critical kinetic uncertainties in modeling hydrogen/carbon monoxide, methane, methanol, formaldehyde, and ethylene combustion. Combust Flame 2018;195:18–29.
[41] Zsély IG, Zádor J, Turányi T. Uncertainty analysis backed development of combustion mechanisms. Proc Combust Inst 2005;30:1273–81.
[42] Li R, He G, Zhang D, Qin F. Skeletal kinetic mechanism generation and uncertainty analysis for combustion of iso-octane at high temperatures. Energy Fuels 2018;32 (3):3842–50.
[43] Hong Y, Dai B, Beck P, Sternin A, Slavinskaya N, Haidn OJ, et al. Development and validation of a reduced chemical kinetic mechanism for CFD simulation of combustion in a GCH_4/GO_2 Combustor. In: In 2018 Joint Propulsion Conference; 2018. p. 4766.
[44] Li T, Hampp F, Lindstedt RP. The impact of hydrogen enrichment on the flow field evolution in turbulent explosions. Combust Flame 2019;203:105–19.
[45] Hampp F, Goh KHH, Lindstedt RP. The reactivity of hydrogen enriched turbulent flames. Process Saf Environ Prot 2020.
[46] Zhang K, Ghobadian A, Nouri JM. Comparative study of non-premixed and partially-premixed combustion simulations in a realistic Tay model combustor. Appl Therm Eng 2017;110:910–20.
[47] Zhang K, Ghobadian A, Nouri JM. Scale-resolving simulation of a propane-fuelled industrial gas turbine combustor using finite-rate tabulated chemistry. Fluids 2020; 5(3):126.
[48] Reichel TG, Paschereit CO. Interaction mechanisms of fuel momentum with flashback limits in lean-premixed combustion of hydrogen. Int J Hydrogen Energy 2017;42(7):4518–29.
[49] Reichel, T.G., Goeckeler, K. and Paschereit, O., 2015. Investigation of lean premixed swirl-stabilized hydrogen burner with axial air injection using oh-plif imaging. In ASME Turbo Expo 2015: Turbine Technical Conference and Exposition (pp. V04AT04A036-V04AT04A036). American Society of Mechanical Engineers.
[50] Borghi R. On the structure and morphology of turbulent premixed flames. In: Recent advances in the Aerospace Sciences. Boston, MA: Springer; 1985. p. 117–38.
[51] Peters N. Laminar flamelet concepts in turbulent combustion. Symposium (International) on Combustion (Vol. 21, No. 1, pp. 1231-1250). Elsevier; 1988.
[52] Terhaar S, Schimek S, Paschereit CO. Combustion of natural gas, hydrogen and bio-fuels at ultra-wet conditions. In: ASME 2011 Turbo Expo: Turbine Technical Conference and Exposition. American Society of Mechanical Engineers Digital Collection; 2011. p. 659–70.